Article

TRANSPARENT PROCESS OPEN ACCESS

THE EMBO JOURNAL

# Mapping early fate determination in Lgr5$^+$ crypt stem cells using a novel *Ki67-RFP* allele

Onur Basak, Maaike van de Born, Jeroen Korving, Joep Beumer, Stefan van der Elst, Johan H van Es & Hans Clevers*

## Abstract

**Cycling Lgr5$^+$ stem cells fuel the rapid turnover of the adult intestinal epithelium. The existence of quiescent Lgr5$^+$ cells has been reported, while an alternative quiescent stem cell population is believed to reside at crypt position +4. Here, we generated a novel *Ki67$^{RFP}$* knock-in allele that identifies dividing cells. Using *Lgr5-GFP;Ki67$^{RFP}$* mice, we isolated crypt stem and progenitor cells with distinct Wnt signaling levels and cell cycle features and generated their molecular signature using microarrays. Stem cell potential of these populations was further characterized using the intestinal organoid culture. We found that Lgr5$^{high}$ stem cells are continuously in cell cycle, while a fraction of Lgr5$^{low}$ progenitors that reside predominantly at +4 position exit the cell cycle. Unlike fast dividing CBCs, Lgr5$^{low}$ Ki67$^-$ cells have lost their ability to initiate organoid cultures, are enriched in secretory differentiation factors, and resemble the Dll1 secretory precursors and the label-retaining cells of Winton and colleagues. Our findings support the cycling stem cell hypothesis and highlight the cell cycle heterogeneity of early progenitors during lineage commitment.**

**Keywords** intestinal stem cells; Ki67; Lgr5; quiescent stem cells; secretory lineage

**Subject Categories** Cell Cycle; Development & Differentiation; Stem Cells

**DOI** 10.15252/embj.201488017 | Received 25 January 2014 | Revised 18 June 2014 | Accepted 10 July 2014 | Published online 4 August 2014

**The EMBO Journal (2014) 33: 2057–2068**

## Introduction

The intestinal epithelium is continuously replenished by stem cells residing at the highly proliferative crypts (Clevers, 2013). Wnt signaling constitutes the major regulator of intestinal homeostasis and its target gene Lgr5 identifies crypt base columnar cells (CBCs) as stem cells (Barker *et al*, 2007). The crypt bottom provides a unique niche that controls stem cell behavior and numbers. Upon loss of contact to their niche, stem cells differentiate into transit-amplifying cells that migrate upward to generate absorptive enterocyte and the secretory goblet, enteroendocrine and tuft cells. Paneth cells localize to the crypt bottom and secrete bactericidal products. They also serve as niche cells that support the neighboring CBCs (Sato *et al*, 2011). Both Paneth cells and the surrounding mesenchyme provide Wnt ligands that—together with Notch signaling—promote stem cell self-renewal (Farin *et al*, 2012). Notch signaling plays a key role during differentiation by inhibiting the secretory fate (van Es *et al*, 2005). BMP signaling forms an inverse gradient with Wnt activity and promotes differentiation of cells that lose contact with their niche (Haramis *et al*, 2004), while EGF/ErbB signaling is a major inducer of proliferation in the crypts (Wong *et al*, 2012).

Lgr5$^+$ CBCs are highly proliferative, yet DNA label retention experiments suggest the presence of slow dividing crypt progenitors as well (Potten *et al*, 1978, 2002; Li & Clevers, 2010). A quiescent multipotent population is suggested to reside at the "+4" position just above the CBCs and express several stem cell markers including Bmi1, Tert and Hopx but has diminished Lgr5 expression (Sangiorgi & Capecchi, 2008; Montgomery *et al*, 2011; Takeda *et al*, 2011; Tian *et al*, 2011; Yan *et al*, 2012). In several studies, Lgr5$^+$ CBC stem cells have been found to share these markers (Itzkovitz *et al*, 2012; Munoz *et al*, 2012; Powell *et al*, 2012; Wong *et al*, 2012; Wang *et al*, 2013). The use of a Histone label retention-based lineage tracing provided evidence for an alternative population, which resides in the crypt, expresses Lgr5 but exclusively generates secretory cells (Buczacki *et al*, 2013). In support, this study shows that some of the Lgr5-expressing CBCs lack cell cycle gene expression. A functionally equivalent population resides prominently at the "+5" position and is enriched in expression of the Notch ligand Delta-like 1 (Dll1) (van Es *et al*, 2012). In the traditional view, differentiation occurs upon exit from the Paneth cell zone, at the so-called "origin of differentiation" around position "= 5" where cells choose between the secretory and absorptive fates (Bjerknes & Cheng, 1981). Inhibition of Notch signaling leads to secretory differentiation of transit-amplifying cells and is coupled to cell cycle exit (van Es *et al*, 2012). However, label-retaining cells (LRCs) are reported within the Paneth cell zone and generate secretory cell types (Buczacki *et al*, 2013). Recent studies in ES cells point out the importance of the cell cycle and lineage commitment, suggesting that lineage commitment might precede differentiation of stem cells (Pauklin & Vallier, 2013).

The intestinal epithelium displays significant plasticity, as the quiescent +4 cells are reported to replenish the CBC pool when

Hubrecht Institute – KNAW and University Medical Centre Utrecht, Utrecht, The Netherlands
*Corresponding author. Tel: +31 30 2121800; E-mail: h.clevers@hubrecht.eu

Lgr5$^+$ cells are selectively killed (Tian *et al*, 2011). Similarly, Dll1$^+$ and label-retaining cells can revert to a stem cell fate upon radiation-mediated loss of proliferating CBCs (van Es *et al*, 2012; Buczacki *et al*, 2013). These results suggest that intestinal crypt populations can be interconverted both during homeostasis and regeneration. To gain insight into the cell cycle dynamics of Lgr5$^+$ CBCs, we have established a system to visualize actively proliferating cells using the proliferation-specific expression of the *mKi67* gene and characterized the early fate choices of intestinal stem cells.

## Results

### Heterogeneous cell cycle dynamics of small intestinal CBCs

In order to understand the cell cycle dynamics of adult intestinal stem cells, we analyzed proliferation of CBCs on intestinal sections of *Lgr5-GFP* mice using double immunofluorescence analysis (Barker *et al*, 2007; Yan *et al*, 2012). KI67 is a nucleolar protein specifically expressed in $G_1$-S-$G_2$-M phases of the cell cycle, but is absent in the $G_0$ phase, making it an excellent marker of proliferation (Hutchins *et al*, 2010). As reported, the vast majority of the Lgr5$^+$ CBCs was proliferating and expressed the cell cycle marker KI67 (88.0 ± 2.0%; Fig 1A and B). However, we observed a small but significant proportion lacking detectable levels of the KI67 protein (Fig 1A). A quiescent stem cell population is proposed to reside at the "+4" position. Lgr5$^+$ KI67$^-$ cells were located throughout the crypt bottom (Fig 1C and D). We quantified the number of Lgr5-, KI67-, and chromogranin A (CHGA)-expressing cells along the crypt axis (see Materials and Methods). Lgr5$^+$ CBCs expressing the enteroendocrine and label-retaining cell marker CHGA have previously been reported as secretory precursors (Sei *et al*, 2011; Buczacki *et al*, 2013). We found that CHGA$^+$ CBCs are concentrated at +3/+4/+5 positions (2.45 ± 0.01), while KI67$^-$ CBCs residing at +1/+4 are CHGA$^-$ (Fig 1C and D). However, the majority of the CHGA$^+$ crypt cells expresses relatively low levels of (if any) Lgr5 and is distributed along the crypt with a peak at +5 position (15.0 ± 5.7% among CHGA$^+$ crypt cells). Lysozyme (LYZ)-expressing Paneth cells were post-mitotic and did not express KI67 (0 ± 0% among LYZ$^+$).

### Ki67$^{RFP}$ marks proliferating cells

In order to visualize actively cell cycling in live cells, we generated a *Ki67$^{RFP}$* knock-in allele by introducing a TagRFP red fluorescent protein in frame at the C-terminus of the Ki67 coding sequence (Fig 2A). As a result, fluorescence is directly linked to the KI67

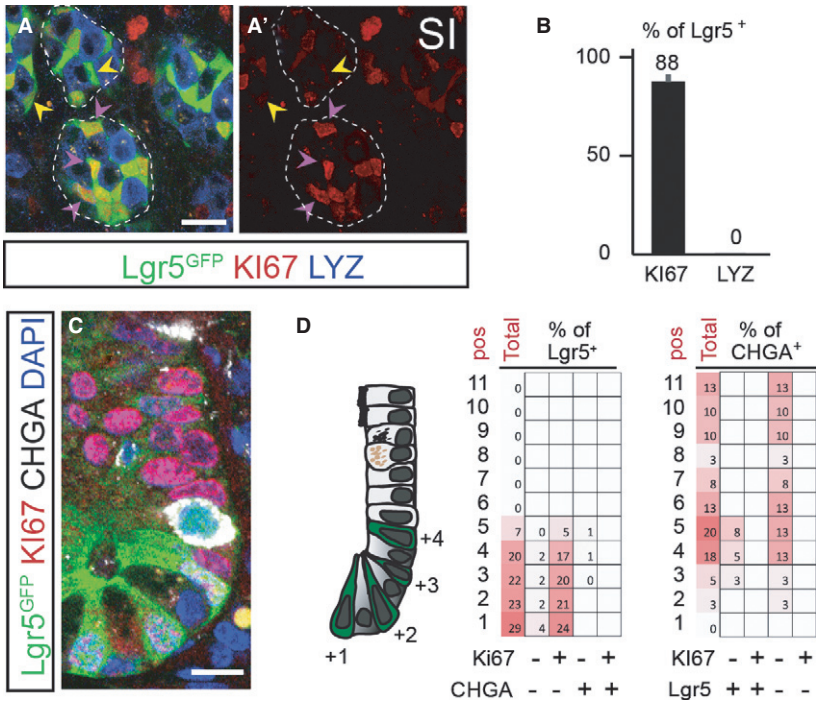


**Figure 1. Characterization of the cell cycle of Lgr5-expressing cells.**

A, B Most of the Lgr5$^+$ (Lgr5-GFP, green) cells have high levels of KI67 (red; white arrowheads) as seen on transverse sections. A small fraction of Lgr5$^+$ stem cells do not express the KI67 protein (yellow arrowheads). Lysozyme (LYZ, blue)-expressing Paneth cells mark the Paneth cell zone and are negative for Lgr5 and KI67. Scale bar, 20 μm. Quantification of the results is shown in (B).

C A cross section of an intestinal crypt showing Lgr5$^+$ stem cells (Green), KI67 (Red), chromogranin A (CHGA, white) and the nucleus (DAPI, blue). Scale bar, 10 μm.

D Quantification of the position of Lgr5$^+$ and CHGA$^+$ cells seen in (C). pos: position, total: sum of Lgr5$^+$ (left) and CHGA$^+$ (right) cells in each position. Each square shows the percentage of cells with a given antigen expression at the respective position among Lgr5$^+$ (left) and CHGA (right)-expressing cells. Lgr5 expression is visualized using the endogenous Lgr5$^{GFP}$ florescence.

 

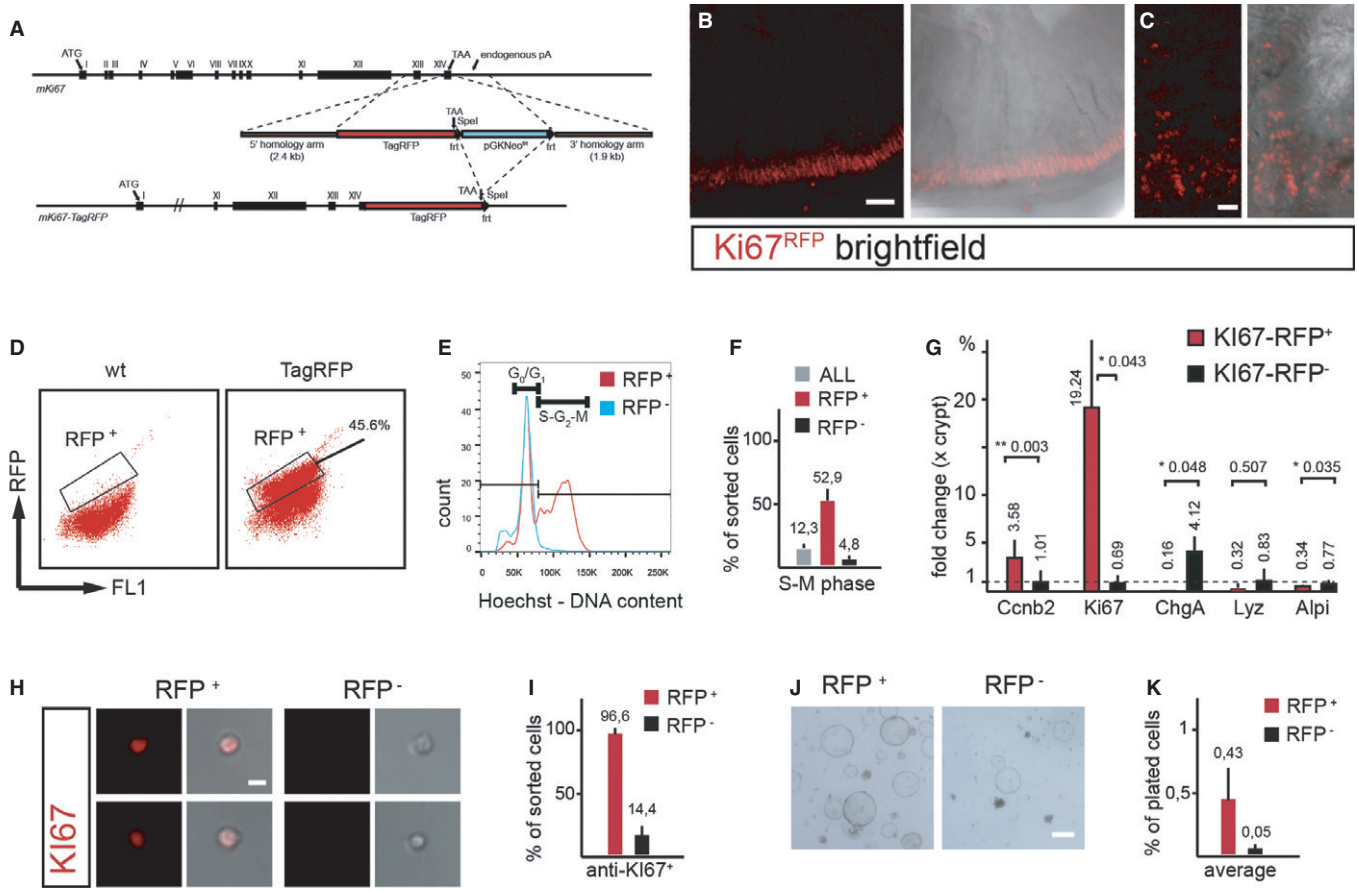


**Figure 2. Generation and characterization of the *Ki67$^{RFP}$* knock-in mouse.**

A The Ki67$^{RFP}$ targeting construct.

B, C Ki67$^{RFP}$ expression can be visualized on live section from the small at low (B) and high (C) magnification.

D RFP-expressing cells from Ki67$^{RFP}$-expressing small intestines can be identified and sorted using FACS.

E, F Graph showing Hoechst 34580 staining on dissociated live intestinal crypt cells. The x-axis shows the dye intensity, which is directly correlated to the DNA content of the cells. Red and blue lines indicate RFP$^+$ and RFP$^-$ fractions, respectively. Quantification of results is shown in (F). All indicates the profile of total live crypt cells.

G Quantitative PCR analysis of sorted Ki67$^{RFP+}$ and Ki67$^{RFP-}$ population. Levels in sorted RFP$^+$ cells is compared to RFP$^-$ cells from the same mouse to indicate the fold change ($n$ = 3). Results are normalized to expression levels in crypt, which is 1.

H, I Sorted single cells were stained using anti-KI67 antibody. RFP$^+$ cells express KI67 while most RFP$^-$ cells lack KI67 expression. Quantification of the results is shown in (I).

J, K Sorted RFP$^+$ cells can initiate organoid cultures while RFP$^-$ cells are less efficient. Quantification of the results is shown in (K).

Data information: Error bars indicate the standard deviation. In (D), FL1 channel is used as a blank channel to visualize autofluorescence. Scale bars: 100 μm (B), 20 μm (C), 10 μm (H), 200 μm (J). In (B) and (C), the gamma settings were adjusted for better visualization of the dim RFP fluorescence.

protein and hence to cell cycle activity. The *Ki67$^{RFP}$* allele was transmitted at the expected Mendelian ratios, and homozygous mice were viable and fertile.

Analysis of TagRFP (RFP) fluorescence on semi-thick vibratome sections from adult mice revealed expression in multiple proliferative tissues, including the spleen, thymus, brain, hair follicle, and colon. For the current study, we focused on the small intestine and characterized RFP expression by fluorescent microscopy and FACS (Fig 2). The fluorescent signal was localized to the crypt as visualized on vibratome sections (Fig 2B and C). In order to find out whether proliferating cells express RFP, we dissociated purified intestinal crypts (Supplementary Fig S1) from the Ki67$^{RFP}$ mice and performed FACS sorting. The DNA content of dissociated live crypt cells from the Ki67$^{RFP}$ mice was measured using Hoechst 34580 (Fig 2D–F) staining. On average, 12.3% (± 3.3) of the crypt cells were in S-M phases of the cell cycle. 52.9% (± 9.8) of the Ki67$^{RFP+}$ cells were in S-M phase of the cell cycle, confirming that RFP expression correlates with cell cycle progression. In sharp contrast, only 4.8% (± 2.5) of the Ki67$^{RFP-}$ cells were in S-M phases of the cell cycle indicating a lack of cell cycle activity (Fig 2E and F). Quantitative PCR analysis revealed a striking enrichment of Ki67 (27.9-fold; 19.2 ± 7.1 versus 0.7 ± 1.0; $P$ = 0.043) and Ccnb2 (3.5-fold; 3.6 ± 1.8 versus 1.0 ± 1.1; $P$ = 0.003) expression in RFP$^+$ fraction compared to the RFP$^-$ cells, supporting proliferation-specific expression of the *Ki67$^{RFP}$* allele (Fig 2G). The enteroendocrine and label-retaining cell marker ChgA (25.9–fold; 0.2 ± 0.1 versus 4.1 ± 1.6; $P$ = 0.048) and the absorptive enterocyte marker Alpi (2.3-fold; 0.3 ± 0.3 versus 0.8 ± 0.3; $P$ = 0.035) were enriched

in the Ki67$^{-}$ fraction, while Lyz levels (2.6-fold; 0.3 ± 0.4 versus 0.8 ± 1.5; $P = 0.5073$) were not statistically different (Fig 2G). In addition, we failed to find any difference in the "+4" marker Bmi1 (1.2-fold; 0.9 ± 0.5 versus 1.0 ± 1.0; $P = 0.842$). Immunostaining analysis using antibodies against the KI67 antigen on sorted RFP populations confirmed RFP$^{+}$ cells express KI67 (96.6 ± 5.6%), while the majority of RFP$^{-}$ cells do not (14.4 ± 7.6%; Fig 2H and I). We concluded that Ki67$^{RFP+}$ cells are actively in the cell cycle, and conversely, the vast majority of dividing cells express the *Ki67$^{RFP}$* allele. Intestinal stem cells are capable of establishing organoid cultures that recapitulate the intestinal epithelium (Sato *et al*, 2009). Sorted RFP$^{+}$ cells robustly initiated organoid cultures (0.43 ± 0.28%), while the RFP$^{-}$ fraction had diminished capacity (0.05 ± 0.04%), suggesting that the majority of the stem cell activity resides within the proliferating epithelial fraction (Fig 2J and K).

### Lgr5$^{+}$ CBCs with distinct cell cycle features can be isolated using the *Lgr5-GFP;Ki67$^{RFP}$* double knock-in mice

We generated *Lgr5-GFP;Ki67$^{RFP}$* double knock-in mice to discriminate cycling and quiescent Lgr5$^{+}$ CBCs. Both reporters were clearly visible on freshly isolated intestinal crypts (Fig 3A). We dissociated small intestinal crypts and performed FACS in an attempt to isolate the Ki67$^{-}$ putative quiescent CBCs. We observed that while most of the Lgr5$^{+}$ cells are cycling, 10.2% (± 1.9%) along the GFP gradient lack Ki67$^{RFP}$ expression consistent with KI67 antigen expression *in vivo* (Fig 3B, K$^{-}$ gates). We have previously identified stem cells and their progeny using GFP expression from the Lgr5 locus (Munoz *et al*, 2012). Here, we focused on stem cells (Lgr5$^{high}$) and their immediate progeny (Lgr5$^{low}$) and we sorted KI67$^{+}$ and KI67$^{-}$ subpopulations. As a result, we describe four populations:

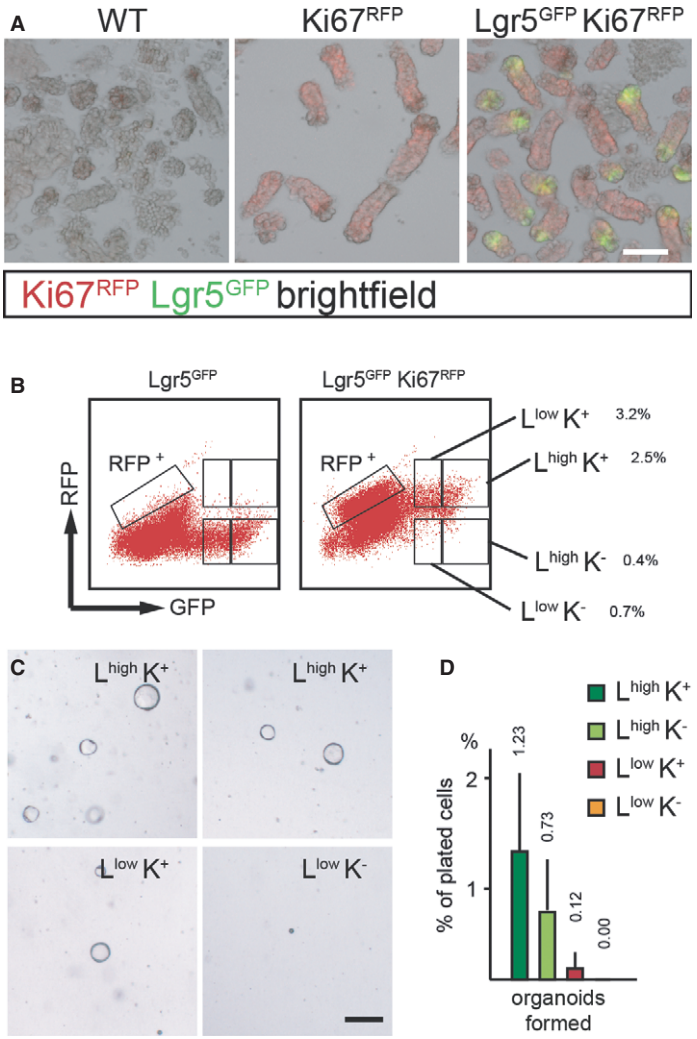


**Figure 3. Identification of CBCs with distinct KI67 expression.**

A Intestinal crypts from control (WT), Ki67$^{RFP}$, and Lgr5$^{GFP}$Ki67$^{RFP}$ mice used for the FACS sorting. Scale bar, 80 μm. The gamma settings were adjusted for better visualization of the dim RFP fluorescence.

B We defined 4 populations of CBCs on FACS using different GFP and RFP expression levels: Lgr5$^{GFP}$ high Ki67$^{RFP}$ positive (L$^{high}$K$^{+}$), Lgr5$^{GFP}$ high Ki67$^{RFP}$ negative (L$^{high}$K$^{-}$), Lgr5$^{GFP}$ low Ki67$^{RFP}$ positive (L$^{low}$K$^{+}$), Lgr5$^{GFP}$ low Ki67$^{RFP}$ negative (L$^{low}$K$^{-}$).

C, D Organoid cultures derived from sorted CBC populations (C) and their quantification (D). Error bars indicate the standard deviation. Scale bar, 80 μm.

Lgr5$^{high}$Ki67$^{+}$ dividing stem cells, Lgr5$^{high}$Ki67$^{-}$ putative quiescent stem cells, Lgr5$^{low}$Ki67$^{+}$ dividing and Lgr5$^{low}$Ki67$^{-}$ putative quiescent crypt progenitors.

We interrogated whether differences in KI67 levels reflect differences in stem cell potential. Lgr5$^{high}$Ki67$^{+}$ and Lgr5$^{high}$Ki67$^{-}$ populations were similarly potent in initiating organoid cultures (single cell plating efficiency 1.23 ± 0.83% and 0.73 ± 0.68%, respectively; Fig 3C and D). Lgr5$^{low}$Ki67$^{+}$ cells initiated culture at lower levels compared to Lgr5$^{high}$ CBCs (0.12 ± 0.17, Fig 3C and D). In sharp contrast, Lgr5$^{low}$Ki67$^{-}$ cells did not display clonogenic ability implying a loss of stemness.

### Global gene expression analysis of CBC populations

To elucidate the molecular features of cycling and quiescent Lgr5$^{+}$ crypt cells, we sorted samples from Lgr5$^{high}$ Ki67$^{+}$ ($n$ = 2), Lgr5$^{high}$ Ki67$^{-}$ ($n$ = 2), Lgr5$^{low}$ Ki67$^{+}$ ($n$ = 4), and Lgr5$^{low}$ Ki67$^{-}$ ($n$ = 2) and generated a global gene expression data set using Affymetrix chips. We compared the gene expression pattern of all 4 populations to document genes differentially expressed between populations using the R2 database (http://r2.amc.nl, AMC, $P < 0.01$, ANOVA test) and identified 1,151 differentially expressed genes (Fig 4A). We compared the molecular signatures of Lgr5$^{high}$ and Lgr5$^{low}$ populations (Fig 4B and C). Expression of Lgr5 (5.2-fold) as well as several genes previously identified as stem cell-specific were enriched more than twofold in GFP$^{high}$ populations (24 among Ki67$^{+}$ and 19 among Ki67$^{-}$) compared to GFP$^{low}$. These included *Tnfrsf19* (Fafilek *et al*, 2013; Stange *et al*, 2013), *Fstl1*, *Nav1*, and *Cttnbp2* (Munoz *et al*, 2012) (Fig 4B and C). We employed the GSEA analysis to evaluate the distribution of the published Lgr5$^{GFPiresCreER+}$ stem cell (Munoz *et al*, 2012) and Wnt (Sansom *et al*, 2004) signature genes between the Lgr5$^{high}$ and Lgr5$^{low}$ populations to confirm the efficiency of our Lgr5$^{GFP}$;Ki67$^{RFP}$ double sorting paradigm to discriminate stem cells from their progeny (Fig 4D). Analysis revealed a high enrichment of both signatures in Lgr5$^{high}$Ki67$^{+}$ (NES: 3.85 and 2.60) as well as Lgr5$^{high}$Ki67$^{-}$ populations (NES: 4.00 and 2.72), validating Lgr5-GFP$^{high}$ cells as stem cells.

### Lgr5$^{high}$ stem cells are continuously in cell cycle

To understand whether the differences in Ki67$^{RFP}$ expression reflects a difference in the cell cycle status of CBC populations, we compared the expression of genes under the GO term "cell cycle" that are statistically different (Fig 5A). 49 genes were differentially expressed including *Ccnb1*, *Cnnb2*, and *AurkA*. Even though RFP$^{+}$ cells express the KI67 protein (Fig 2), we observed that the mKi67

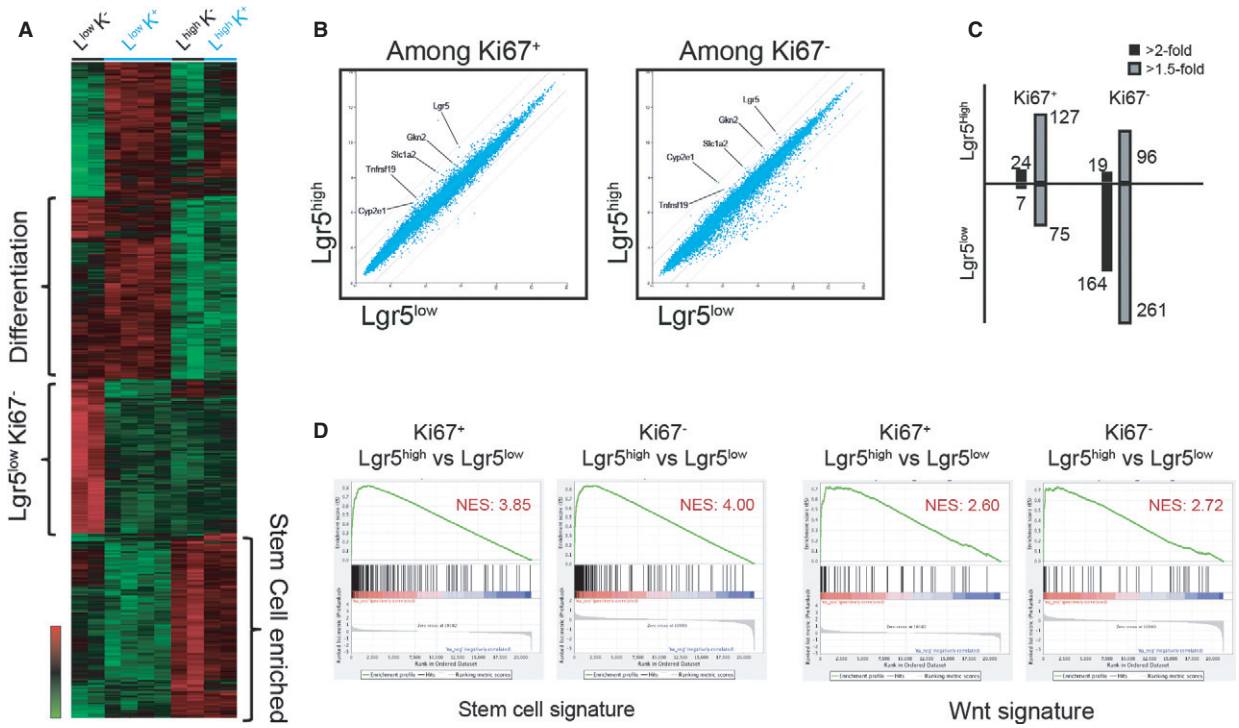


**Figure 4. Comparison of CBC populations.**

A Heatmap generated using the differentially expressed genes between CBC populations calculated as significantly different (ANOVA test, $P < 0.01$). Red indicates higher expression.

B Two-group plotters comparing Ki67$^{+}$Lgr5$^{high}$ to Ki67$^{+}$Lgr5$^{low}$ (left) and Ki67$^{-}$Lgr5$^{high}$ to Ki67$^{-}$Lgr5$^{low}$ (right).

C Quantification of the number of genes that are significantly different (ANOVA, $P < 0.01$) between groups and is expressed at least twofold (black bars) of 1.5-fold higher (gray bars) in one of the groups.

D Gene set enrichment analysis (GSEA) reveals high similarity between the top 200 stem cell genes (Munoz *et al*, 2012) and 58 genes upregulated upon deletion of APC in the small intestine (Sansom *et al*, 2004) to the genes enriched in Ki67$^{+}$Lgr5$^{high}$ versus Ki67$^{+}$Lgr5$^{low}$ and Ki67$^{-}$Lgr5$^{high}$ versus Ki67$^{-}$Lgr5$^{low}$. Results are displayed in log2.

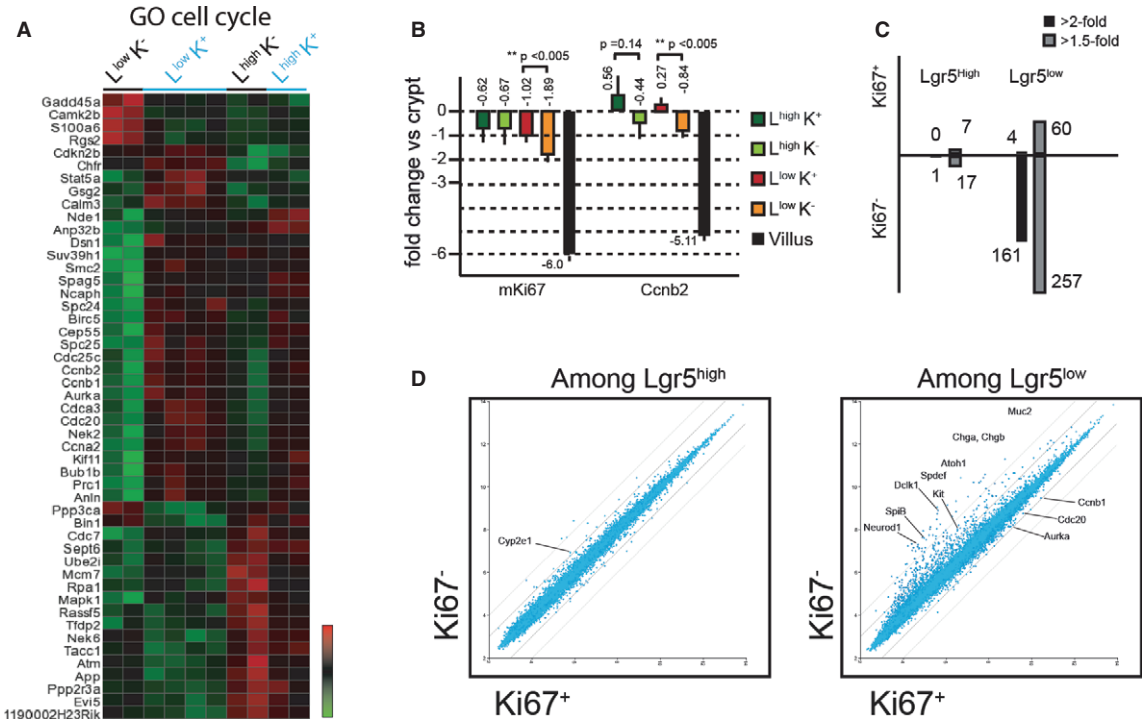


**Figure 5. The cell cycle dynamics of CBC populations.**

A Heatmap displaying genes with the combined GO term "cell cycle" that are differentially expressed between CBC populations (ANOVA test, $P < 0.01$). Red indicates higher expression.

B qPCR analysis for the expression of cell cycle indicators mKi67 and Ccnb2 in CBC populations, crypt, and the villus. Results are normalized to the expression level in the crypt, which is displayed as 0. Error bars indicate the standard deviation.

C Quantification of the number of genes that are significantly different (ANOVA, $P < 0.01$) between groups and is expressed at least twofold (black bars) of 1.5-fold higher (gray bars) in one of the groups.

D Two-group plotters comparing Lgr5$^{high}$Ki67$^{+}$ to Lgr5$^{high}$Ki67$^{-}$ (left) and Lgr5$^{low}$Ki67$^{+}$ to Lgr5$^{low}$Ki67$^{-}$ (right).

RNA was not significantly enriched in any of the CBC populations. qPCR analysis confirmed that *mKi67* and *Ccnb2* genes were expressed at strikingly higher levels in all Lgr5 populations compared to the villus where most cells are terminally differentiated. Their expression was not significantly different between the two groups of Lgr5$^{high}$ stem cells but was significantly less in Lgr5$^{low}$Ki67$^{-}$ cells compared to the Lgr5$^{low}$Ki67$^{+}$ cells consistent with the microarray data (Fig 5A and B). In agreement with their shared organoid-initiating ability, Lgr5$^{high}$Ki67$^{+}$ and Lgr5$^{high}$Ki67$^{-}$ stem cells displayed a very high correlation in their gene expression pattern (Fig 5C and D). The low number of genes that are differentially expressed between Lgr5$^{high}$Ki67$^{+}$ (0 gene > twofold and seven genes over 1.5-fold) and Lgr5$^{high}$Ki67$^{-}$ (1 gene > twofold and 17 genes > 1.5-fold) suggests that the populations are functionally identical (Fig 5C and D). Differences were much more pronounced between Lgr5$^{low}$Ki67$^{+}$ (four genes > twofold and 60 genes over 1.5-fold) and Lgr5$^{low}$Ki67$^{-}$ (161 genes > twofold and 257 genes over 1.5-fold) populations (Fig 5C and D). Based on the overlap in their molecular signatures of Lgr5$^{high}$Ki67$^{+}$ and Lgr5$^{high}$Ki67$^{-}$ populations, enrichment of stem cell genes and high levels of expression of cell cycle-related genes, we suggest that both classes of Lgr5$^{high}$ intestinal stem cells are continuously cycling. Lgr5$^{low}$Ki67$^{-}$ cells display a distinct cell cycle pattern intermediate between other Lgr5 populations and differentiated cells.

### Lgr5$^{low}$Ki67$^{-}$ cells are early secretory precursors

To better understand the program controlling self-renewal and differentiation, we focused on the 61 genes annotated to have "transcription factor", "transcription regulator activity", or "transcriptional repressor activity" and are differentially expressed among Lgr5 populations (Fig 6A). Among those, 24 were enriched in Lgr5$^{high}$ cells (*Zfp202, Maged1, Lbh, Cbfb, Ctnnb1, Smad5, Zscan2, Fem1b, Tcfap2, Tfdp2, Tcf7, Brca2, Sox4, Trim24, Ehf, Dach1, Gtf2i, Notch1, Atoh8, Mycl1, Atm, Bclaf1, Nr2e3,* and *Ascl2*) including *Ascl2*, a major regulator of stem cell identity (Fig 6A) (van der Flier *et al*, 2009). We identified 20 transcription factors in the Lgr5$^{low}$Ki67$^{-}$ population (*Foxj2, Runx1, Prox1, Foxa3, Mxd4, Hmx2, Pou2f3, SpiB, Pax6, Nkx2-2, St18, Pax4, Neurod1, Isl1, Runx1t1, Creb3 l4, Fev, Spdef, Neurog3,* and *Atoh1*) including *Atoh1*, a master regulator of secretory differentiation (Yang *et al*, 2001; van Es *et al*, 2005; Shroyer *et al*, 2007). Several factors implicated in secretory differentiation were in this group. *Pax4, NeuroD1, Nkx2-2,* and *Isl1* are inducers of endocrine differentiation, while *Spdef* is required for both the Paneth and goblet cell differentiation (Naya *et al*, 1997; Larsson *et al*, 1998; Jenny *et al*, 2002; Desai *et al*, 2008; Gregorieff *et al*, 2009). *SpiB* is an important player in differentiation of M cells, which are derived from Lgr5$^{+}$ stem cells, but are rare in the intact intestine (Kanaya *et al*, 2012; de Lau *et al*, 2012). As Lgr5$^{low}$Ki67$^{-}$

 

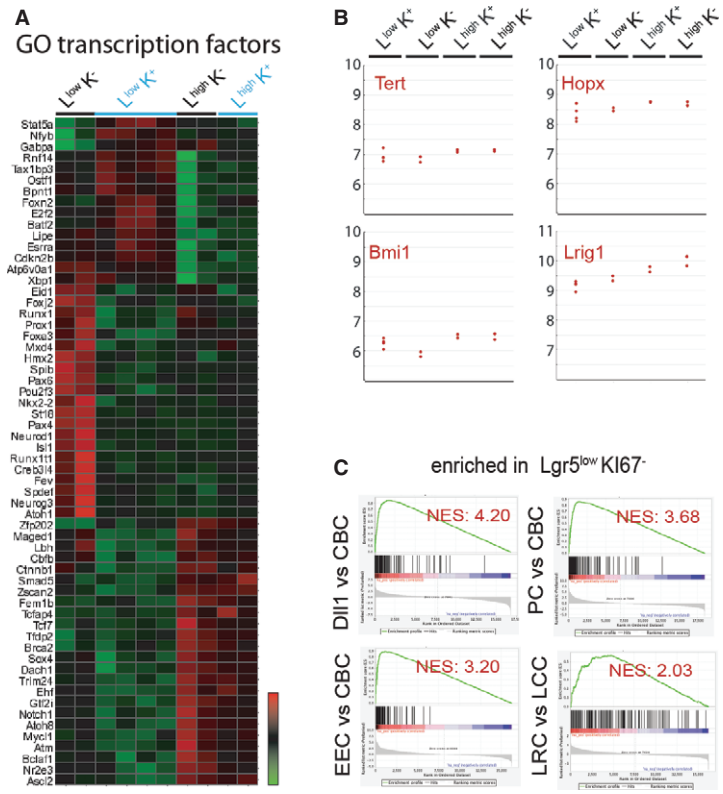


**Figure 6. Lgr5$^{low}$Ki67$^{-}$ population corresponds to the secretory precursors.**

A Heatmap displaying genes with the combined GO terms "transcription factor" and "transcriptional regulatory activity" that are differentially expressed between CBC populations (ANOVA test, $P < 0.01$). Red indicates higher expression.

B Plots displaying the distribution of the proposed quiescent stem cell markers to CBC populations. The numbers on the *y*-axis show the normalized expression values on microarrays in log2. Each dot represents a separate sample.

C Gene set enrichment analysis (GSEA) analysis. Genes significantly enriched in Lgr5$^{low}$Ki67$^{-}$ population was used to generate a molecular signature, which was compared to published data sets including the Dll1$^{+}$ (van Es *et al*, 2012), Paneth (PC; van Es *et al*, 2012), enteroendocrine (EEC; van Es *et al*, 2012) and label-retaining cell (LRC; Buczacki *et al*, 2013) expression profiles. NES: Normalized enrichment score.

cells express significantly higher levels of ChgA (7.0-fold more than Lgr5$^{low}$Ki67$^{+}$ and 6.2-fold more than Lgr5$^{high}$Ki67$^{-}$, Supplementary Fig S2) and likely represent the +4/5 cells, we analyzed the expression of reported quiescent stem cell markers. Tert, Hopx, and Bmi1 were not significantly higher in any of the populations while Lrig1 was expressed slightly higher in Lgr5$^{high}$ cells excluding them as specific markers of a slow-dividing CBC population (Fig 6B) (Montgomery *et al*, 2011; Yan *et al*, 2012; Wong *et al*, 2012). This confirms several recent reports on the shared expression of these markers between slow-cycling "+4" cells and Lgr5 CBC cells (Itzkovitz *et al*, 2012; Munoz *et al*, 2012; Powell *et al*, 2012; Wong *et al*, 2012; Wang *et al*, 2013).

Lgr5 subpopulations also displayed a distinct profile of signaling pathway components. Inhibition of Notch signaling results in an upregulation of Atoh1 expression and induces secretory differentiation. Consistently, *Notch1* mRNA was high in stem cells and was virtually absent in Lgr5$^{low}$Ki67$^{-}$ cells. Another Lgr5$^{low}$Ki67$^{-}$-enriched gene, *St18*, is a tumor suppressor that during pancreatic development inhibits Notch signaling (Wang *et al*, 2007). The notion of secretory differentiation in Lgr5$^{low}$Ki67$^{-}$ cells is supported by other factors highly enriched in this population. Enteroendocrine markers ChgA and ChgB, as well as hormones expressed by enteroendocrine subtypes (Stt, Gcg) and some of their regulators (Rfx6), are the most prominent factors (Supplementary Fig S2A). Confocal and qPCR analysis confirmed that some of the Lgr5$^{+}$ cells express ChgA (Supplementary Fig S2B–D) as well as somatostatin (Stt) (Supplementary Fig S2D). Similarly, *Kit* and *Muc2*, Paneth and goblet cell factors, respectively, are also among the enriched genes (Supplementary Fig S2A). Taken together, the results imply that the Lgr5$^{low}$Ki67$^{-}$ cells are in the secretory lineage.

Lgr5$^{+}$ stem cells generate secretory cells through intermediate populations, that is the Dll1$^{+}$ "+5" cells and Winton's slow dividing/label-retaining cells (van Es *et al*, 2012; Buczacki *et al*, 2013). To investigate the relationship of Lgr5$^{low}$Ki67$^{-}$ cells with the proposed secretory precursors and related intestinal populations, we used the GSEA analysis (Fig 6C). We compared the genes significantly enriched in Lgr5$^{low}$Ki67$^{-}$ cells to the ranked gene lists of Paneth cells, enteroendocrine cells, Dll1 cells (van Es *et al*, 2012), and label-retaining cells (Buczacki *et al*, 2013) (see Materials and Methods). We employed the normalized enrichment score (NES) as a mean to evaluate their similarity to each population. Lgr5$^{low}$Ki67$^{-}$ population was most similar to the Dll1$^{+}$ population, followed by the Paneth cells, enteroendocrine cells, and the label-retaining cells (Fig 6C; NES: 4,20, 3,68, 3,20, respectively). These results imply

that the Lgr5$^{low}$Ki67$^{-}$ population represents the described secretory progenitor populations.

#### Lgr5$^{-}$ Ki67$^{-}$ crypt cells display a differentiated cell signature

Lgr5 is gradually down-regulated early during differentiation. In order to analyze Lgr5$^{-}$ crypt populations with distinct cell cycle features, we generated the *Ki67$^{RFP}$;Lgr5$^{GFPDTR}$* double knock-in mice, where GFP is expressed by every Lgr5$^{+}$ cell (Tian *et al*, 2011). We isolated Lgr5$^{-}$ Ki67$^{+}$ (Lgr5$^{-}$ K$^{+}$) and Lgr5$^{-}$Ki67$^{-}$ (Lgr5$^{-}$K$^{-}$) populations and analyzed the differences in their gene expression pattern using qPCR (Supplementary Fig S3). *Lgr5* mRNA expression was constantly enriched in Lgr5$^{GFPDTR}$ sorted cells on average by 32-fold (28.7 ± 14.1 versus 0.9 ± 0.3). As expected, proliferation markers Ki67 (16.8 ± 13.4) and Ccnb2 (2.50 ± 0.85) were highly enriched in Lgr5$^{-}$ K$^{+}$ compared to Lgr5$^{-}$ K$^{-}$ population. Transcription factors regulating secretory differentiation, Atoh1 (0.04 ± 0.04) and NeuroD1 (0.01 ± 0.00), were exclusively expressed in Lgr5$^{-}$ K$^{-}$ cells, consistent with an inverse correlation between secretory differentiation and cell cycle progression. Paneth cell marker lysozyme (Lyz; 0.29 ± 0.15), the goblet cell marker Gob5 (0.09 ± 0.04), and the enteroendocrine/secretory progenitor marker chromagranin A (ChgA; 0.01 ± 0.00) were similarly enriched in non-dividing Lgr5$^{-}$ crypt fraction. We observed an enrichment of Fabp2 (0.46 ± 0.01) and Alpi (0.44 ± 0.12) in Lgr5$^{-}$ K$^{-}$ cells compared to the Lgr5$^{-}$ K$^{+}$ population. Both of these genes are upregulated in enterocytes upon differentiation and are expressed at lower levels in the crypt. Finally, even though we cannot exclude a rare quiescent population with high levels of Bmi1 expression, we failed to detect a correlation between cell cycle progression and Bmi1 expression, which is slightly higher in Lgr5$^{-}$ K$^{-}$ cells (0.59 ± 0.02).

## Discussion

We generated a model where proliferating cells can be genetically identified, visualized and isolated for molecular and cellular analysis. The *Ki67$^{RFP}$* allele is specifically expressed in dividing cells at all cell cycle phases and can be used to dissect specific populations into proliferating and quiescent sub-fractions. GFP expressing stem cell reporters are available for several organs where *Ki67$^{RFP}$* is expressed (e.g. brain, hair follicles), making it a valuable tool for the stem cell community.

We performed the first analysis in one of the best-characterized somatic stem cell systems, the intestinal crypts, where proliferation must be tightly controlled to maintain stem cell numbers as well as the required output of differentiating daughter cells. The number of divisions that a fast cycling intestinal stem cell undergoes during mammalian life is high. For this reason, it has been assumed that an upstream/alternative stem cell population exists that has exited the cell cycle into quiescence. We isolated CBC populations using Lgr5 as an indicator of stemness and KI67 protein expression as an indicator of cell cycle progression. Our results indicate that Lgr5$^{high}$ stem cells display little variation in their cell cycle dynamics. Even though a KI67$^{-}$ population exists, its global expression pattern mimics that of the dividing stem cells. This is further supported by high expression of Ki67 and Ccnb2 in both Lgr5 populations. These levels are similar to the crypt average and much higher than that of the differentiated villus cells. Furthermore, both populations can efficiently initiate organoid cultures displaying comparable "stemness". We conclude that Lgr5$^{high}$ CBC stem cells are continuously in the cell cycle. The difference in fluorescence levels of the *Ki67$^{RFP}$* allele may reflect a Gaussian distribution in a uniformly cycling population. Alternatively, a transient exit from the cell cycle after mitosis could result in the absence of the KI67 protein in Lgr5$^{+}$ cells that soon continue to proliferate. We have observed that a percentage of RFP$^{-}$ cells express the KI67 protein supporting a gap period during the maturation of the TagRFP protein or its accumulation during the re-entry into the cell cycle.

The Lgr5$^{low}$Ki67$^{-}$ cells, however, display an intermediate characteristic with significantly less cell cycle gene expression compared to both types of Lgr5$^{high}$ stem cells and Lgr5$^{low}$Ki67$^{+}$ cells. Lgr5$^{low}$Ki67$^{-}$ cells reside in the differentiation zone and their expression pattern closely resembles that of the LRCs (Buczacki *et al*, 2013) and the Dll1$^{+}$ cells (Stamataki *et al*, 2011; van Es *et al*, 2012). In agreement to their similarity to the LRCs, CHGA expressing Lgr5$^{low}$Ki67$^{-}$ cells are distributed in the crypt with a peak at +4/5. It is likely that Lgr5$^{low}$Ki67$^{-}$ population overlaps with both LRCs and Dll1$^{+}$ progenitors (Fig 7). Lgr5$^{low}$ cells stall in the cell cycle and down-regulate Ki67 expression on transition from dividing stem cells into the slow dividing secretory progenitors. LRC cells can persist for days prior to differentiation into enteroendocrine or Paneth cells. Goblet cells and tuft cells rarely arise from LRCs and are likely direct descendants of Dll1$^{+}$ cells (Stamataki *et al*, 2011; van Es *et al*, 2012; Buczacki *et al*, 2013). Lgr5$^{low}$Ki67$^{+}$ cells lose their stem cell signature, maintain Notch receptor expression and lack transcription factors implicated in secretory differentiation. Even though we cannot exclude the contribution of Lgr5$^{low}$Ki67$^{-}$ cells, it is tempting to speculate that the Lgr5$^{low}$Ki67$^{+}$ are the main intermediate between the stem cells and enterocytes.

Our experiments indicate that the proliferating cells are much more efficient in organoid forming potential than quiescent cells. Lgr5$^{high}$ cells are highly proliferative and efficient in initiating organoid cultures. Albeit less efficiently, Lgr5$^{low}$ cells can also be induced to generate organoids. Both Dll1$^{+}$ cells and LRCs retain some proliferative capacity and occasionally reenter the cell cycle becoming KI67$^{+}$. This could potentially explain why unlike the label-retaining or Dll1$^{+}$ secretory precursors, Lgr5$^{low}$Ki67$^{-}$ cells do not readily generate organoids. A feasible alternative is the lack of regeneration cues that drives secretory cell proliferation upon injury in our organoid culture.

The biological meaning behind the connection of cell cycle exit and secretory differentiation is intriguing. Enterocytes in the villus are more numerous compared to the secretory cells. The differences in the proliferation rate between secretory and enterocyte precursors would maintain the correct ratio of absorptive to secretory lineages. During genotoxic conditions, such as viral infection or inflammation, secretory precursors could constitute a reserve stem cells population that is long-lived and protected from accumulation of replicative stress and mutations. The regenerative capacity of the relatively quiescent secretory progenitors as seen by Buczacki *et al* (2013) and van Es *et al* (2012) suggests that reversion from relative quiescence into a fast cycling stem cell fate is a physiological phenomenon. A standing question is how this transition is controlled. As differences in Lgr5 levels reflect differences in Wnt signaling activity, high level of which is required for organoid

 

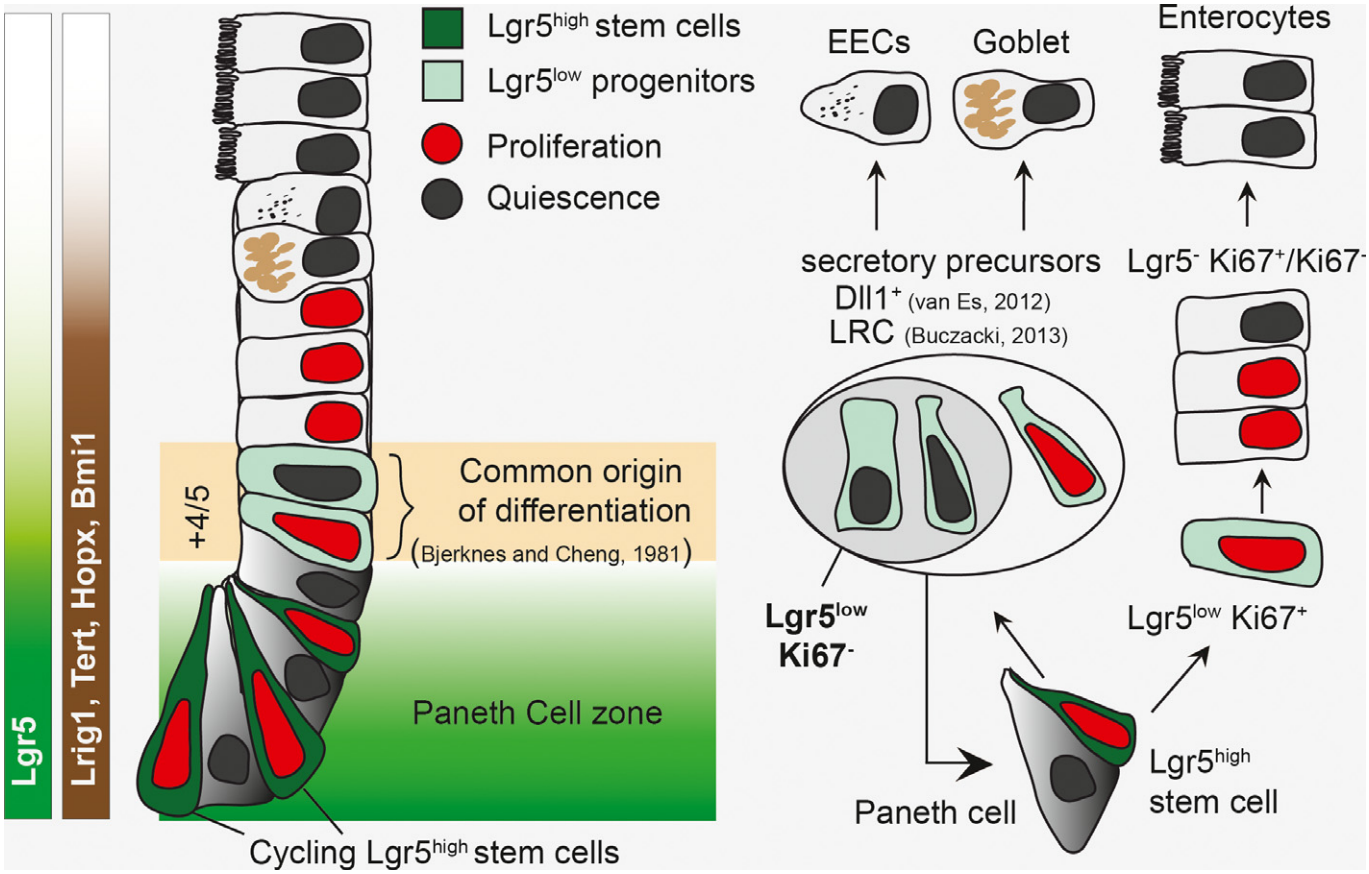


**Figure 7. Stem and progenitor cell compartmentalization in the small intestine.**
Paneth cells mark the stem cell zone where dividing Lgr5$^{high}$ stem cells reside. In the "zone of differentiation", progenitors are specified to the absorptive or the secretory lineages (Bjerknes & Cheng, 1981). The "+4" markers are shared between both Lgr5$^{high}$ stem cells and Lgr5$^{low}$ progenitors independent of their cell cycle status. Lgr5$^{low}$Ki67$^{-}$ intermediate secretory precursors arise from Lgr5$^{high}$ stem cells and overlap with Dll1$^{+}$ cells, the common precursors of the Paneth, goblet, and the enteroendocrine cells (van Es *et al*, 2012). The label-retaining cells are the longest-lived secretory precursors that differentiate into Paneth and enteroendocrine cells (Buczacki *et al*, 2013). Both LRCs and Dll1$^{+}$ can re-enter the cell cycle to generate multiple secretory cells, displaying limited proliferation potential (secretory precursors, red nucleus). Partially overlapping secretory precursors likely represent different maturational stages. Lgr5$^{low}$Ki67$^{+}$ cells rapidly proliferate and generate enterocytes through Lgr5$^{-}$Ki67$^{+}$ and/or Lgr5$^{-}$Ki67$^{-}$ transient amplifying progenitors. Dark and light green indicate high and low Lgr5 expression, respectively. Red nucleus: mitotically active state; black nucleus: $G_0$ state.

formation, Wnt signaling is an attractive candidate (Sato *et al*, 2009; van Es *et al*, 2012). Myc is a major downstream effector of Wnt, which promotes proliferation during intestinal regeneration (Ireland *et al*, 2004; Muncan *et al*, 2006; Sansom *et al*, 2007). In support, constitutive activation of Wnt signaling and NF-kB signaling induces dedifferentiation in the intestine (Schwitalla *et al*, 2013). Constitutive activation of Ras signaling enhances intestinal stem cell proliferation, which in combination with Apc activation can induce dedifferentiation of intestinal villi (Schwitalla *et al*, 2013; Snippert *et al*, 2014). Inhibition of Notch signaling is a known inducer of secretory differentiation, which coincides with decreased crypt proliferation (van Es *et al*, 2005). Whether activation of Notch signaling in the secretory precursors is enough for their conversion or additional signals activated in response to injury would instruct their dedifferentiation remains to be explored.

Previous efforts to identify an alternative stem cell population to CBCs focused on label-retaining cells mainly residing directly above the Paneth cell zone. The high similarity in the global expression pattern of Dll1 cells, LRCs, and Lgr5$^{low}$Ki67$^{-}$ cells strongly suggests that the GFP$^{low}$ population in our analysis includes these +4/5 positions. The fact that the four "classical" markers for "+4" cells are expressed by these Lgr5$^{low}$Ki67$^{-}$ cells implies that these cells most likely represent the proposed quiescent "+4" stem cells as identified in the original lineage tracing studies using *Bmi1*, *Tert*, *Hopx*, and *Lrig1* (Sangiorgi & Capecchi, 2008; Montgomery *et al*, 2011; Takeda *et al*, 2011; Yan *et al*, 2012). Our observations are entirely consistent with those of Winton and colleagues and imply that a slowly cycling population of secretory precursor cells resides around position "+4" and expresses the markers Hopx, Bmi1, Tert, and Lrig1 in combination with intermediate levels of Lgr5. These precursors are normally destined to differentiate into Paneth and enteroendocrine cells, but have the capacity to revert to a CBC stem cell upon tissue damage. Thus, these cells—when taken at the individual level—do not represent long-lived stem cells. Yet, the pool of these quiescent cells that is constantly replenished functionally constitutes a "reserve" stem cell population, to be called into action upon damage. Our findings using a novel knock-in system to directly visualize KI67-expressing cycling cells provide support for the dividing stem cell hypothesis and suggest that the "+4" population represents slow dividing secretory precursors.

## Materials and Methods

### Generation of the *Ki67$^{RFP}$* knock-in mouse and the animals used

*Ki67$^{RFP}$* knock-in mouse was generated by homologous recombination in embryonic stem cells by targeting a TagRFP cassette at the stop codon of the *mKi67* gene. The endogenous stop codon is deleted to generate a C-terminal fusion of the KI67 protein with the TagRFP red fluorescent protein (Merzlyak *et al*, 2007). Details of embryonic stem cell targeting, Lgr5$^{GFPiresCreER}$ (Barker *et al*, 2007) and Lgr5$^{GFPDTR}$ (Tian *et al*, 2011) mice were described elsewhere. Mice were maintained within the animal facilities at the Hubrecht Institute, and experiments were performed according to the national rules and regulations of the Netherlands.

### FACS sorting

Freshly isolated small intestines of *Ki67$^{RFP}$* and *Lgr5$^{GFP}$* mice were incised along their length, and villi were removed by scraping. The tissue was then washed 5 times in PBS by vigorous shaking to remove the access mucus. After incubation in PBS/EDTA (2 mM) for 15 min, gentle shaking removed remaining villi and intestinal tissue was subsequently incubated in 5 mM PBS/EDTA for 30 min at 4°C. Vigorous shaking yielded free crypts that were filtered through a 100-μm mesh and incubated in PBS supplemented with Trypsin (10 mg/ml; Sigma) and DNase (0.8 mg/ml; Roche) for 15 min at 37°C. Subsequently, cells were spun down, resuspended in SMEM (Invitrogen) and filtered through a 40-μm mesh. GFP- and TagRFP-expressing cells were isolated using BD FACSAria II cell sorter (BD Biosciences). Approximately 100,000 cells from a combination of 5–8 mice were sorted per population for each experiment. All analyzed populations were collected simultaneously.

### Cell culture analysis

FACS-sorted intestinal crypt populations were collected in the intestinal culture medium including Wnt3a (50% conditioned medium) supplemented with the ROCK inhibitor Y-27632 (Sigma Aldrich) as described (Sato *et al*, 2009). The basic culture medium (advanced Dulbecco's modified Eagle's medium/F12 supplemented with penicillin/streptomycin, 10 mM HEPES, Glutamax, B27 [Life Technologies, Carlsbad, CA] and 1 mM N-acetylcysteine [Sigma]) was supplemented with 50 ng/ml murine recombinant epidermal growth factor (EGF; Peprotech, Hamburg, Germany), R-spondin1 (conditioned medium, 5% final volume), and Noggin (conditioned medium, 5% final volume). Conditioned media were produced using HEK293T cells stably transfected with HA-mouse Rspo1-Fc (gift from Calvin Kuo, Stanford University) or after transient transfection with mouse Noggin-Fc expression vector. Advanced Dulbecco's modified Eagle's medium/F12 supplemented with penicillin/streptomycin, and Glutamax was conditioned for 1 week. Wnt3a conditioned medium was produced using stably transfected L cells after 1 week of conditioning in medium (as previously described Sato *et al*, 2009) containing 10% fetal bovine serum. Cells were plated in matrigel (BD Bioscience) and cultured for a week before the number of organoids was quantified. At least 10,000 cells for Ki67$^{RFP}$ and 1,000 cells for Lgr5$^{GFP}$Ki67$^{RFP}$ double sorts were used per population per experiment. Experiments were done in biological duplicates.

### Tissue preparation and immunofluorescence analysis

Fresh isolated Ki67$^{RFP}$ small intestinal samples were embedded in 4% low melting agarose (Invitrogen) and cut by a vibrating microtome (HM650, Microm) in cold medium and visualized immediately after for immunofluorescence analysis. Due to dim fluorescence and increase in the background, we could not analyze the TagRFP expression after formaldehyde fixation. Lgr5$^{GFP}$ small intestinal samples were fixed in 4% paraformaldehyde overnight, processed in 30% sucrose overnight and frozen in tissue freezing medium (Jung) on dry ice. 100-μm-thick floating sections were prepared using a cryostat (Cryostar NX70, Thermo scientific). Sections were blocked with 2% normal donkey serum (Jackson ImunoResearch) for 1 h at RT, permeabilized in PBS supplemented with 0.5% Triton X-100 overnight and stained with the indicated primary antibody. Primary antibodies used were eFluor-660 conjugated rat anti-KI67 (1:1,000; eBioscience), rabbit anti-lysozyme (1:3,000; DAKO), goat anti-chromogranin A (1:500, Santa Cruz) and rabbit anti-somatostatin (1:500; Invitrogen). Subsequently, sections were incubated with the corresponding secondary antibodies Alexa568 conjugated anti-rabbit and anti-goat antibodies (1:1,000; Molecular Probes) in blocking buffer containing DAPI (1:1,000, Invitrogen) for 2 h at RT and embedded using Vectashield (Vector Labs). Sections were imaged with Sp5 and Sp8 confocal microscopes (Leica) and processed using Photoshop CS5 and ImageJ software. Isolated intestinal crypts were visualized using the EVOS microscope (Electron Microscopy Sciences). The position of Lgr5$^+$ and ChgA$^+$ cells were quantified on *z*-stacks spanning the entire depth of the quantified crypts. For Fig 1B, 221 Lgr5$^+$ cells from biological duplicates were quantified. For Fig 1D, in total, 32 crypts from biological duplicates were quantified. The Lgr5$^+$ cell at the bottom of the crypt was considered position +1.

### Microarray analysis, bioinformatics, and quantitative PCR

The Affymetrix analysis was performed on a genome-wide mRNA expression platform (Mouse Gene ST 1.1 arrays). The expression data extracted from the raw files were MAS5-normalized with the RMA-sketch algorithm from Affymetrix Power Tools and log2-transformed. Data were analyzed using the R2 web application, which is freely available at http://r2.amc.nl. In total, 21,212 unique genes are represented on the array. For genes represented with multiple probes, the one with the highest average expression level across the arrays was used. Expression levels were averaged within each group of arrays (Lgr5$^{high}$Ki67$^+$, Lgr5$^{high}$Ki67$^-$, Lgr5$^{low}$Ki67$^+$, and Lgr5$^{low}$Ki67$^-$) and log2 ratios calculated. Genes differentially expressed among groups were calculated according to the level of significance ($P < 0.01$; ANOVA). The Gene Set Enrichment Analysis (GSEA) was performed using the freely available software (v.2.0, Broad Institute; Subramanian *et al*, 2005) using preranked lists of mean expression changes and input signatures that were derived from published microarray data (Sansom *et al*, 2004; van Es *et al*, 2012; Munoz *et al*, 2012; Heijmans *et al*, 2013). qPCR analysis was performed using the SYBR-Green and Bio-Rad systems as described (Munoz *et al*, 2012).

 

### Accession numbers

Array data are available at Gene Expression Omnibus (GEO) under the accession number GSE52813 (http://www.ncbi.nlm.nih.gov/geo/query/acc.cgi?token=etodgcqynfmfzib&acc=GSE52813).

**Supplementary information** for this article is available online: http://emboj.embopress.org


### Acknowledgements

We would like to thank Richard Volckmann, Jan Koster, Richard van Voort, and Peter van Sluis for the excellent support with the microarrays and bioinformatics analysis, Drs. Henner Farin, Meritxell Huch and Bon-Kyoung Koo for the fruitful discussion. This work was supported in part by grants by the Cancer Genomics Center (CGCII) to O.B., KWF/PF-HUBR 2007-3956 to M.v.d.B. and EU/232814-StemCellMark to J.H.v.E.


### Author contributions

OB and HC conceived, designed, and analyzed the experiments. OB constructed the *Ki67*$^{RFP}$ mouse, analyzed the microarray data, and performed the cell culture and qPCR experiments. SVDE and OB designed and performed the FACS experiments. JB was supervised by OB and performed the confocal microscopy analysis. MVDB has provided the technical assistance of the mouse experiments. JK has performed the ES cell injections. Data interpretation was aided by JHVE. Funding was provided by HC. The manuscript was written by OB and HC and commented on by all other authors.

### Conflict of interest

The Hubrecht Institute holds several patents related to Lgr5.

## References


Barker N, van Es JH, Kuipers J, Kujala P, van den Born M, Cozijnsen M, Haegebarth A, Korving J, Begthel H, Peters PJ, Clevers H (2007) Identification of stem cells in small intestine and colon by marker gene Lgr5. *Nature* 449: 1003–1007

Bjerknes M, Cheng H (1981) The stem-cell zone of the small intestinal epithelium. V. Evidence for controls over orientation of boundaries between the stem-cell zone, proliferative zone, and the maturation zone. *Am J Anat* 160: 105–112

Buczacki SJ, Zecchini HI, Nicholson AM, Russell R, Vermeulen L, Kemp R, Winton DJ (2013) Intestinal label-retaining cells are secretory precursors expressing Lgr5. *Nature* 495: 65–69

Clevers H (2013) The intestinal crypt, a prototype stem cell compartment. *Cell* 154: 274–284

Desai S, Loomis Z, Pugh-Bernard A, Schrunk J, Doyle MJ, Minic A, McCoy E, Sussel L (2008) Nkx2.2 regulates cell fate choice in the enteroendocrine cell lineages of the intestine. *Dev Biol* 313: 58–66

van Es JH, van Gijn ME, Riccio O, van den Born M, Vooijs M, Begthel H, Cozijnsen M, Robine S, Winton DJ, Radtke F, Clevers H (2005) Notch/gamma-secretase inhibition turns proliferative cells in intestinal crypts and adenomas into goblet cells. *Nature* 435: 959–963

van Es JH, Sato T, van de Wetering M, Lyubimova A, Nee AN, Gregorieff A, Sasaki N, Zeinstra L, van den Born M, Korving J, Martens AC, Barker N, van Oudenaarden A, Clevers H (2012) Dll1$^{+}$ secretory progenitor cells revert to stem cells upon crypt damage. *Nat Cell Biol* 14: 1099–1104

Fafilek B, Krausova M, Vojtechova M, Pospichalova V, Tumova L, Sloncova E, Huranova M, Stancikova J, Hlavata A, Svec J, Sedlacek R, Luksan O, Oliverius M, Voska L, Jirsa M, Paces J, Kolar M, Krivjanska M, Klimesova K, Tlaskalova-Hogenova H *et al* (2013) Troy, a tumor necrosis factor receptor family member, interacts with lgr5 to inhibit wnt signaling in intestinal stem cells. *Gastroenterology* 144: 381–391

Farin HF, Van Es JH, Clevers H (2012) Redundant sources of Wnt regulate intestinal stem cells and promote formation of Paneth cells. *Gastroenterology* 143: 1518–1529 e1517

van der Flier LG, van Gijn ME, Hatzis P, Kujala P, Haegebarth A, Stange DE, Begthel H, van den Born M, Guryev V, Oving I, van Es JH, Barker N, Peters PJ, van de Wetering M, Clevers H (2009) Transcription factor achaete scute-like 2 controls intestinal stem cell fate. *Cell* 136: 903–912

Gregorieff A, Stange DE, Kujala P, Begthel H, van den Born M, Korving J, Peters PJ, Clevers H (2009) The ets-domain transcription factor Spdef promotes maturation of goblet and Paneth cells in the intestinal epithelium. *Gastroenterology* 137: 1333–1345 e1331–1333

Haramis AP, Begthel H, van den Born M, van Es J, Jonkheer S, Offerhaus GJ, Clevers H (2004) *De novo* crypt formation and juvenile polyposis on BMP inhibition in mouse intestine. *Science* 303: 1684–1686

Heijmans J, van Lidth de Jeude JF, Koo BK, Rosekrans SL, Wielenga MC, van de Wetering M, Ferrante M, Lee AS, Onderwater JJ, Paton JC, Paton AW, Mommaas AM, Kodach LL, Hardwick JC, Hommes DW, Clevers H, Muncan V, van den Brink GR (2013) ER stress causes rapid loss of intestinal epithelial stemness through activation of the unfolded protein response. *Cell Rep* 3: 1128–1139

Hutchins JR, Toyoda Y, Hegemann B, Poser I, Heriche JK, Sykora MM, Augsburg M, Hudecz O, Buschhorn BA, Bulkescher J, Conrad C, Comartin D, Schleiffer A, Sarov M, Pozniakovsky A, Slabicki MM, Schloissnig S, Steinmacher I, Leuschner M, Ssykor A *et al* (2010) Systematic analysis of human protein complexes identifies chromosome segregation proteins. *Science* 328: 593–599

Ireland H, Kemp R, Houghton C, Howard L, Clarke AR, Sansom OJ, Winton DJ (2004) Inducible Cre-mediated control of gene expression in the murine gastrointestinal tract: effect of loss of beta-catenin. *Gastroenterology* 126: 1236–1246

Itzkovitz S, Lyubimova A, Blat IC, Maynard M, van Es J, Lees J, Jacks T, Clevers H, van Oudenaarden A (2012) Single-molecule transcript counting of stem-cell markers in the mouse intestine. *Nat Cell Biol* 14: 106–114

Jenny M, Uhl C, Roche C, Duluc I, Guillermin V, Guillemot F, Jensen J, Kedinger M, Gradwohl G (2002) Neurogenin3 is differentially required for endocrine cell fate specification in the intestinal and gastric epithelium. *EMBO J* 21: 6338–6347

Kanaya T, Hase K, Takahashi D, Fukuda S, Hoshino K, Sasaki I, Hemmi H, Knoop KA, Kumar N, Sato M, Katsuno T, Yokosuka O, Toyooka K, Nakai K, Sakamoto A, Kitahara Y, Jinnohara T, McSorley SJ, Kaisho T, Williams IR *et al* (2012) The Ets transcription factor Spi-B is essential for the differentiation of intestinal microfold cells. *Nat Immunol* 13: 729–736

Larsson LI, St-Onge L, Hougaard DM, Sosa-Pineda B, Gruss P (1998) Pax 4 and 6 regulate gastrointestinal endocrine cell development. *Mech Dev* 79: 153–159

de Lau W, Kujala P, Schneeberger K, Middendorp S, Li VS, Barker N, Martens A, Hofhuis F, DeKoter RP, Peters PJ, Nieuwenhuis E, Clevers H (2012) Peyer's patch M cells derived from Lgr5(+) stem cells require SpiB and are induced by RankL in cultured "miniguts". *Mol Cell Biol* 32: 3639–3647

Li L, Clevers H (2010) Coexistence of quiescent and active adult stem cells in mammals. *Science* 327: 542–545

Merzlyak EM, Goedhart J, Shcherbo D, Bulina ME, Shcheglov AS, Fradkov AF, Gaintzeva A, Lukyanov KA, Lukyanov S, Gadella TW, Chudakov DM (2007) Bright monomeric red fluorescent protein with an extended fluorescence lifetime. *Nat Methods* 4: 555 – 557

Montgomery RK, Carlone DL, Richmond CA, Farilla L, Kranendonk ME, Henderson DE, Baffour-Awuah NY, Ambruzs DM, Fogli LK, Algra S, Breault DT (2011) Mouse telomerase reverse transcriptase (mTert) expression marks slowly cycling intestinal stem cells. *Proc Natl Acad Sci USA* 108: 179 – 184

Muncan V, Sansom OJ, Tertoolen L, Phesse TJ, Begthel H, Sancho E, Cole AM, Gregorieff A, de Alboran IM, Clevers H, Clarke AR (2006) Rapid loss of intestinal crypts upon conditional deletion of the Wnt/Tcf-4 target gene c-Myc. *Mol Cell Biol* 26: 8418 – 8426

Munoz J, Stange DE, Schepers AG, van de Wetering M, Koo BK, Itzkovitz S, Volckmann R, Kung KS, Koster J, Radulescu S, Myant K, Versteeg R, Sansom OJ, van Es JH, Barker N, van Oudenaarden A, Mohammed S, Heck AJ, Clevers H (2012) The Lgr5 intestinal stem cell signature: robust expression of proposed quiescent "+4" cell markers. *EMBO J* 31: 3079 – 3091

Naya FJ, Huang HP, Qiu Y, Mutoh H, DeMayo FJ, Leiter AB, Tsai MJ (1997) Diabetes, defective pancreatic morphogenesis, and abnormal enteroendocrine differentiation in BETA2/neuroD-deficient mice. *Genes Dev* 11: 2323 – 2334

Pauklin S, Vallier L (2013) The cell-cycle state of stem cells determines cell fate propensity. *Cell* 155: 135 – 147

Potten CS, Hume WJ, Reid P, Cairns J (1978) The segregation of DNA in epithelial stem cells. *Cell* 15: 899 – 906

Potten CS, Owen G, Booth D (2002) Intestinal stem cells protect their genome by selective segregation of template DNA strands. *J Cell Sci* 115: 2381 – 2388

Powell AE, Wang Y, Li Y, Poulin EJ, Means AL, Washington MK, Higginbotham JN, Juchheim A, Prasad N, Levy SE, Guo Y, Shyr Y, Aronow BJ, Haigis KM, Franklin JL, Coffey RJ (2012) The pan-ErbB negative regulator Lrig1 is an intestinal stem cell marker that functions as a tumor suppressor. *Cell* 149: 146 – 158

Sangiorgi E, Capecchi MR (2008) Bmi1 is expressed *in vivo* in intestinal stem cells. *Nat Genet* 40: 915 – 920

Sansom OJ, Reed KR, Hayes AJ, Ireland H, Brinkmann H, Newton IP, Batlle E, Simon-Assmann P, Clevers H, Nathke IS, Clarke AR, Winton DJ (2004) Loss of Apc *in vivo* immediately perturbs Wnt signaling, differentiation, and migration. *Genes Dev* 18: 1385 – 1390

Sansom OJ, Meniel VS, Muncan V, Phesse TJ, Wilkins JA, Reed KR, Vass JK, Athineos D, Clevers H, Clarke AR (2007) Myc deletion rescues Apc deficiency in the small intestine. *Nature* 446: 676 – 679

Sato T, Vries RG, Snippert HJ, van de Wetering M, Barker N, Stange DE, van Es JH, Abo A, Kujala P, Peters PJ, Clevers H (2009) Single Lgr5 stem cells build crypt-villus structures *in vitro* without a mesenchymal niche. *Nature* 459: 262 – 265

Sato T, van Es JH, Snippert HJ, Stange DE, Vries RG, van den Born M, Barker N, Shroyer NF, van de Wetering M, Clevers H (2011) Paneth cells constitute the niche for Lgr5 stem cells in intestinal crypts. *Nature* 469: 415 – 418

Schwitalla S, Fingerle AA, Cammareri P, Nebelsiek T, Goktuna SI, Ziegler PK, Canli O, Heijmans J, Huels DJ, Moreaux G, Rupec RA, Gerhard M, Schmid R, Barker N, Clevers H, Lang R, Neumann J, Kirchner T, Taketo MM, van den Brink GR *et al* (2013) Intestinal tumorigenesis initiated by dedifferentiation and acquisition of stem-cell-like properties. *Cell* 152: 25 – 38

Sei Y, Lu X, Liou A, Zhao X, Wank SA (2011) A stem cell marker-expressing subset of enteroendocrine cells resides at the crypt base in the small intestine. *Am J Physiol Gastrointest Liver Physiol* 300: G345 – G356

Shroyer NF, Helmrath MA, Wang VY, Antalffy B, Henning SJ, Zoghbi HY (2007) Intestine-specific ablation of mouse atonal homolog 1 (Math1) reveals a role in cellular homeostasis. *Gastroenterology* 132: 2478 – 2488

Snippert HJ, Schepers AG, van Es JH, Simons BD, Clevers H (2014) Biased competition between Lgr5 intestinal stem cells driven by oncogenic mutation induces clonal expansion. *EMBO Rep* 15: 62 – 69

Stamataki D, Holder M, Hodgetts C, Jeffery R, Nye E, Spencer-Dene B, Winton DJ, Lewis J (2011) Delta1 expression, cell cycle exit, and commitment to a specific secretory fate coincide within a few hours in the mouse intestinal stem cell system. *PLoS ONE* 6: e24484

Stange DE, Koo BK, Huch M, Sibbel G, Basak O, Lyubimova A, Kujala P, Bartfeld S, Koster J, Geahlen JH, Peters PJ, van Es JH, van de Wetering M, Mills JC, Clevers H (2013) Differentiated troy(+) chief cells act as reserve stem cells to generate all lineages of the stomach epithelium. *Cell* 155: 357 – 368

Subramanian A, Tamayo P, Mootha VK, Mukherjee S, Ebert BL, Gillette MA, Paulovich A, Pomeroy SL, Golub TR, Lander ES, Mesirov JP (2005) Gene set enrichment analysis: a knowledge-based approach for interpreting genome-wide expression profiles. *Proc Natl Acad Sci USA* 102: 15545 – 15550

Takeda N, Jain R, LeBoeuf MR, Wang Q, Lu MM, Epstein JA (2011) Interconversion between intestinal stem cell populations in distinct niches. *Science* 334: 1420 – 1424

Tian H, Biehs B, Warming S, Leong KG, Rangell L, Klein OD, de Sauvage FJ (2011) A reserve stem cell population in small intestine renders Lgr5-positive cells dispensable. *Nature* 478: 255 – 259

Wang S, Zhang J, Zhao A, Hipkens S, Magnuson MA, Gu G (2007) Loss of Myt1 function partially compromises endocrine islet cell differentiation and pancreatic physiological function in the mouse. *Mech Dev* 124: 898 – 910

Wang F, Scoville D, He XC, Mahe MM, Box A, Perry JM, Smith NR, Lei NY, Davies PS, Fuller MK, Haug JS, McClain M, Gracz AD, Ding S, Stelzner M, Dunn JC, Magness ST, Wong MH, Martin MG, Helmrath M *et al* (2013) Isolation and characterization of intestinal stem cells based on surface marker combinations and colony-formation assay. *Gastroenterology* 145: 383 – 395 e381–321

Wong VW, Stange DE, Page ME, Buczacki S, Wabik A, Itami S, van de Wetering M, Poulsom R, Wright NA, Trotter MW, Watt FM, Winton DJ, Clevers H, Jensen KB (2012) Lrig1 controls intestinal stem-cell homeostasis by negative regulation of ErbB signalling. *Nat Cell Biol* 14: 401 – 408

Yan KS, Chia LA, Li X, Ootani A, Su J, Lee JY, Su N, Luo Y, Heilshorn SC, Amieva MR, Sangiorgi E, Capecchi MR, Kuo CJ (2012) The intestinal stem cell markers Bmi1 and Lgr5 identify two functionally distinct populations. *Proc Natl Acad Sci USA* 109: 466 – 471

Yang Q, Bermingham NA, Finegold MJ, Zoghbi HY (2001) Requirement of Math1 for secretory cell lineage commitment in the mouse intestine. *Science* 294: 2155 – 2158